

Triboelectric Nanogenerator Network Integrated with Charge Excitation Circuit for Effective Water Wave Energy Harvesting

Xi Liang, Tao Jiang, Yawei Feng, Pinjing Lu, Jie An, and Zhong Lin Wang*

Ocean waves are considered to be one of the most promising renewable energy sources, and harvesting such energy via triboelectric nanogenerators (TENGs) is an effective strategy toward large-scale blue energy. However, most previous optimization schemes of TENG cannot meet the demands of practical applications. In this work, a new charge excitation circuit (CEC) with advantages of integration, high efficiency, and minimum impedance is developed specially for TENGs to harvest water wave energy. The TENG with the CEC exhibits significantly improved output performance, with a maximum power of 25.8 mW and power density of 49.3 W m⁻³, and a 208 times enhanced current of 25.1 mA is achieved. Furthermore, a scheme of integrating TENG network and CECs is proposed for realizing large-scale wave energy harvesting. The charge excitation TENG network is demonstrated to successfully power a digital thermometer and a wireless communication system with mobile phone through transmitting radio frequency (RF) signals for remote environmental monitoring. This study not only offers a strategy to greatly enhance the output performance of TENG networks in water wave energy harvesting, but also provides useful guidance for constructing maritime communication platform based on blue energy toward a maritime internet of things system.

1. Introduction

With the rapid development of human society and economy, people are more and more aware of the importance of environmental protection. Recently, the exploitation of clean and renewable energy sources to replace the fossil fuels has become the focus of scientific research around the world.^[1] Ocean, occupying 70% of the earth surface area, contains tremendous energies which deserve to be developed.^[2,3] However, it is still difficult to capture ocean energy and put it into practical applications at present despite the great efforts invested. So far, the common method of harvesting ocean energy is based on the electromagnetic generators (EMGs), which are bulky, costly, easily eroded, and not suitable to work under the low frequency of the ocean.^[4,5] Hence, other more effective ways are in urgent need of research.

Triboelectric nanogenerator (TENG, also called as Wang generator) proposed by Wang in 2012 has provided a new route toward developing ocean energy.^[6] Compared with EMGs relying on the electromagnetic induction, the physical mechanisms of TENGs is based on the Maxwell's displacement current, and the TENGs are more adaptable to the low-frequency of <2 Hz.^[7–11] In addition, the TENGs also exhibit other advantages such as low cost, light weight,^[12] easy fabrication, and high power density,^[13,14] so they have attracted a wide range of attention in many fields including the exploitation of ocean wave energy.^[15–24] In order to improve the output performance of TENGs, previous researches have been focused on rational structural design, materials selection, surface modification, and so on.^[18,25–32] However, these methods can only increase the outputs to some extent due to the low and unstable charge density on the tribo-surfaces.^[33] Recently, the reported external-charge pumping method and self-charge excitation system provide promising and effective strategies for achieving high-output TENGs toward practical applications.^[33–35] Therefore, it is of important research significance to devise reasonable charge excitation circuit system and combine it with TENGs for harvesting water wave energy more efficiently.

In this work, we developed a new charge excitation system based on the voltage-multiplying circuit (VMC), specially for

X. Liang, Prof. T. Jiang, Y. Feng, P. Lu, J. An, Prof. Z. L. Wang
CAS Center for Excellence in Nanoscience
Beijing Key Laboratory of Micro-nano Energy and Sensor
Beijing Institute of Nanoenergy and Nanosystems
Chinese Academy of Sciences
Beijing 100083, P. R. China
E-mail: zlwang@gatech.edu

X. Liang, Prof. T. Jiang, Y. Feng, J. An, Prof. Z. L. Wang
School of Nanoscience and Technology
University of Chinese Academy of Sciences
Beijing 100049, P. R. China

Prof. T. Jiang, P. Lu
Center on Nanoenergy Research
School of Physical Science and Technology
Guangxi University
Nanning, Guangxi 530004, P. R. China

Prof. Z. L. Wang
School of Materials Science and Engineering
Georgia Institute of Technology
Atlanta, GA 30332, USA

 The ORCID identification number(s) for the author(s) of this article can be found under <https://doi.org/10.1002/aenm.202002123>.

DOI: 10.1002/aenm.202002123

TENGs that collect water wave energy. Not only the output performance of a single TENG was increased by multiple times, but also a scheme was proposed to realize high-output TENG network through integrating with the charge excitation circuits (CEC). First, the working principle of the charge excitation TENG was clarified in details by analyzing the voltage of each part in this circuit system, and the basic performance of the system was measured at the same time. Next, in real water waves, the influences of water wave frequency and amplitude on the outputs of the TENG integrated with the CEC were systematically investigated. Then, a hexagonal TENG network with seven charge excitation TENG units was fabricated and tested under different water wave conditions. Finally, the charge excitation TENG network was applied to power a digital thermometer and a wireless communication system with a mobile phone through transmitting radio frequency (RF) signals, demonstrating the important role of the CEC in expanding the potential applications of TENGs in remote maritime environmental monitoring.

2. Results and Discussion

A new charge excitation circuit was developed to integrate with a TENG for improving its output performance in water wave energy harvesting. The spherical TENG with spring-assisted multilayered structure reported in our previous work was chosen as an example, because of its optimized output performance and efficiency.^[36] The specific structure of the TENG, floating on the ocean surface, is schematically presented in **Figure 1a**, and the multilayered structure inside it is shown in Figure S1, Supporting Information. When connecting with the CEC, the alternating output current of the TENG can be not only increased by many times, but also transformed into direct currents (DC). Several spherical TENG units are, respectively, integrated with the CECs, and then directly linked with each other in parallel without rectified bridges, forming a charge excitation TENG network. Here, a hexagonal TENG network with the CECs was fabricated, whose photograph is exhibited in Figure 1b.^[21] Taking a hexagonal TENG network as a

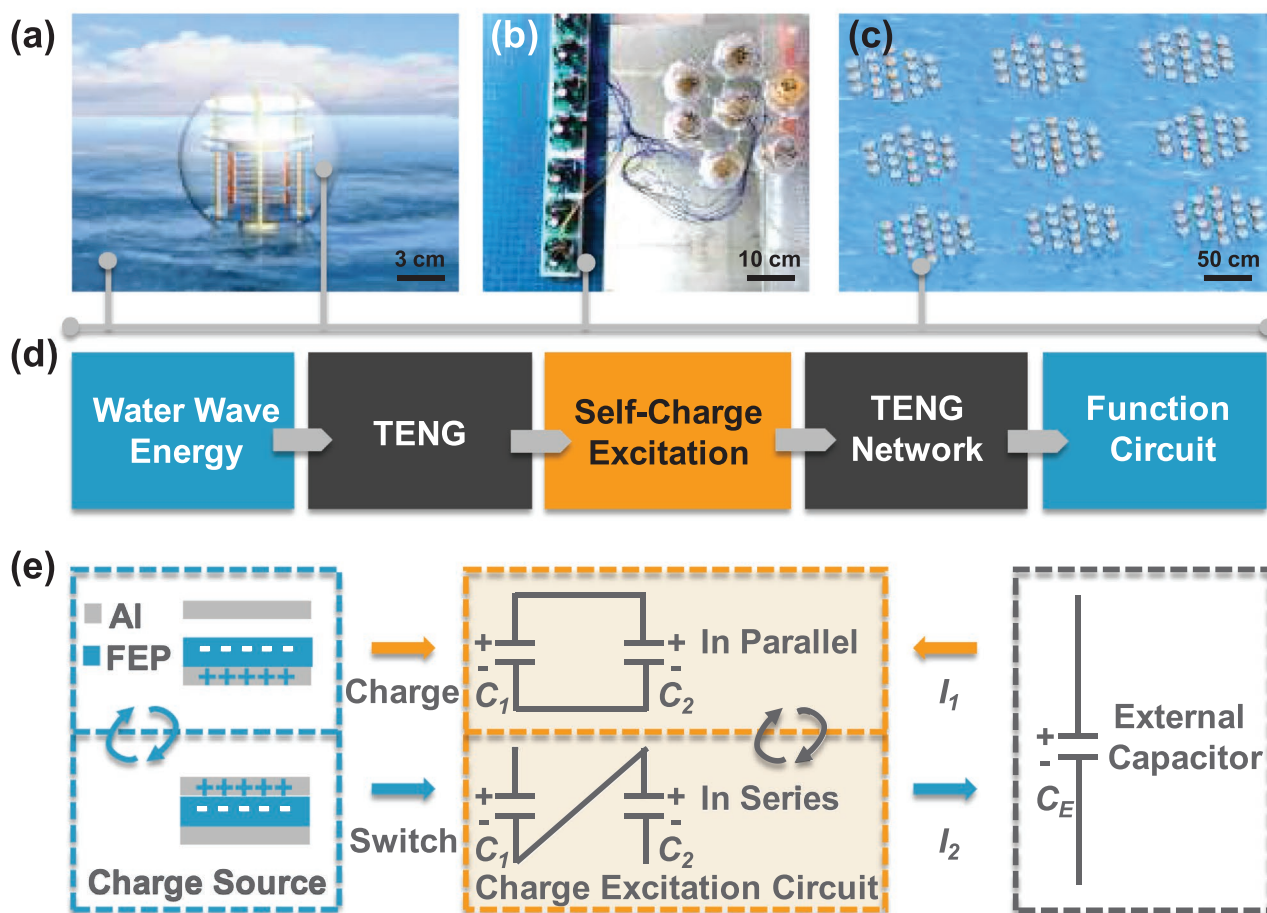


Figure 1. a) Schematic diagram of a single spherical TENG with spring-assisted multilayered structure floating on the ocean surface. b) Photograph of an as-fabricated hexagonal TENG network floating on the water surface, which is composed of seven spherical TENG units linked by rigid strings and connected by the charge excitation circuits. c) Schematic illustration of a multi-module TENG network for large-scale blue energy harvesting. d) Framework for the self-powered system achieved by the charge excitation TENG network driven by the water wave motions. e) Working principle of a contact-separation TENG integrated with the CEC.

module, a multi-module TENG network is also proposed for large-scale blue energy harvesting, as schematically depicted in Figure 1c.^[37] Figure 1d illustrates a framework for a self-powered system achieved by the charge excitation TENG network. The TENG network with enhanced performance by the CECs harvests the water wave energy effectively and the DC outputs can power various functional circuits, such as sensing, alarming, displaying, transmitting signals, and so on, greatly expanding the application range of TENGs for ocean energy harvesting.

The working principle of a charge excitation TENG is demonstrated in Figure 1e. Here, a TENG of the contact-separation mode was applied as the charge source of the system, for example. Actually, the CEC is also suitable for TENGs at other modes. The CEC is a capacitor group constituted by two identical capacitors C_1 and C_2 (10 μF), which can be autonomously switched from the parallel to series connection. During the separation process of the TENG, these two capacitors are charged in parallel, while in the contacting process, the TENG no longer charges the capacitors but switches their connection manner to be in series, doubling the voltage of the capacitor group. With this method, the triboelectric charges generated by the TENG are stored in the capacitors, and the voltage of the capacitor group is controlled by the TENG, breaking the limitation of the charge density on the tribo-surfaces. To implement a complete loop circuit, an external capacitor C_E (1 mF) was introduced in this system, which is also powered by the TENG. If C_E is 10 μF equal to C_1 and C_2 , not only there will be less charge flowing in the system, but also the voltage difference between the capacitors group and C_E will shrink. Since the capacitance of C_E is much larger than that of the capacitor group, the voltage of the capacitor group almost always keeps consistent with C_E . Initially, the capacitor group is in the parallel connection, so the voltage values on the C_1 , C_2 , and C_E are all the same. As the connection of the capacitor group is changed to be in series, the respective voltage value on the C_1 and C_2 has to become as half of that on the C_E , and the voltage drop will cause charge transfer from C_1 and C_2 to C_E . Afterward, the connection type of the capacitor group is switched to be in parallel again, so the voltage on the C_1 and C_2 must rise to match C_E , making the charges flow from C_E back to the capacitor group and constituting a cycle of charge transfer. Concluding, after the voltage change of each capacitor reaches a steady state, C_1 and C_2 in series charge C_E , while C_1 and C_2 in parallel are charged by C_E , where the charge transfer enables objective output currents, greatly increasing the output performance of TENG.

To achieve automatic circuit switch, metal-oxide-semiconductor field effect transistors (MOSFET) were employed in this system, including two N-type MOSFETs (denoted by M_1 , M_3) and one P-type MOSFET (denoted by M_2), and the detailed circuit diagram of this system is depicted in Figure 2a. Although the open-circuit voltage of the TENG is quite high, the real voltage on the MOSFETs is much lower than it and unable to break the MOSFETs. For satisfying the demands of large-scale TENG network in future,^[37] the electrical components were integrated on a square circuit board (4 cm \times 4 cm), whose photograph is displayed in Figure S2, Supporting Information. When the spherical TENG vibrates at 0.5 Hz and the voltage of C_E is stabilized at 6 V, the voltage that the TENG inputs into the system is shown in Figure 2b. During the positive input,

from the enlarged view in the lower part of Figure 2b, M_1 is off, while M_2 and M_3 are on. The simplified circuit diagram in this period is described in Figure S3a, Supporting Information, where the dashed lines represent the open-circuit states, indicating that the TENG and C_E charge the capacitor group C_1 and C_2 in parallel. The voltage drop on the C_1 and C_2 is exhibited in Figure 2c, and this charging process of C_1 , C_2 from 3.3 to 6 V is marked in the enlarged view in the lower part of Figure 2c. The current output in this process (Output 1) was measured in the upper part of Figure 2d, whose direction is also pointed out. Conversely, in the process of negative input, M_1 is turned on, while M_2 and M_3 are turned off simultaneously, causing C_1 and C_2 to become in series connection and charge C_E , which is depicted in Figure S3b, Supporting Information. The voltage on the C_1 and C_2 within this process declines from 6 to 3.3 V (Figure 2c), and the output current (Output 2) and its direction are also presented in Figure 2d. It is apparent that the output current of the TENG integrated with the CEC is significantly increased, with a peak value above 20 mA. The amount of transferred charges corresponding to one current peak was measured to be over 25.5 μC (Figure S4, Supporting Information), which is 35 times higher than the initial value of 0.7 μC .^[36]

The peak current and peak power-resistance relationships of the TENG with the CEC were investigated, as shown in Figure 2e, exhibiting the maximum power of 32.1 mW at the matched resistance of 500 Ω . Not only the output power is increased by three times, but also the matched resistance is reduced from 2.21 M Ω to 500 Ω , implying that the restriction of large impedance and unbalanced load match of the TENG is effectively resolved.^[36] Generally, the capacitance of TENG is very low, leading to high equivalent internal impedance. Here, the integrating of the CEC greatly increases the capacitance, and the equivalent internal impedance of TENG declines accordingly. Therefore, the matched resistance in this work is reduced. The charging performance of the charge excitation TENG to various capacitors is presented in Figure S5a, Supporting Information. The comparison between the managed charging using the CEC and direct charging to a 1 mF capacitor was made in Figure S5b, Supporting Information, indicating that the charging speed can be improved by up to seven times. The improvement is because the TENG with the CEC can provide larger amount of transferred charges per cycle. The normal operation of the charge excitation system requires C_E to maintain a certain voltage value, so the TENG has to first charge C_E , which is presented in the left part of Figure 2f. The relevant output currents with C_E charged to different voltage values are shown in the right side of Figure 2f. When the voltage value on the C_E is equal to 2 V, the system is unable to work, since the gate-source voltage V_{GS} controlled by the voltage on the C_E cannot turn on M_2 and M_3 . As the voltage on the C_E rises, the voltage on the C_1 and C_2 increases, leading to magnification of the output current. However, the trend of current is not linear but gradually stabilized because of the large leakage current when C_E is charged to a higher level.

In order to quantify the output performance of the TENG with the CEC, the TENG was tested in a standard wave tank equipment,^[18] which was built to simulate real ocean waves in the laboratory stage, and the scene of a single TENG vibrating under the water wave triggering is schematically depicted in

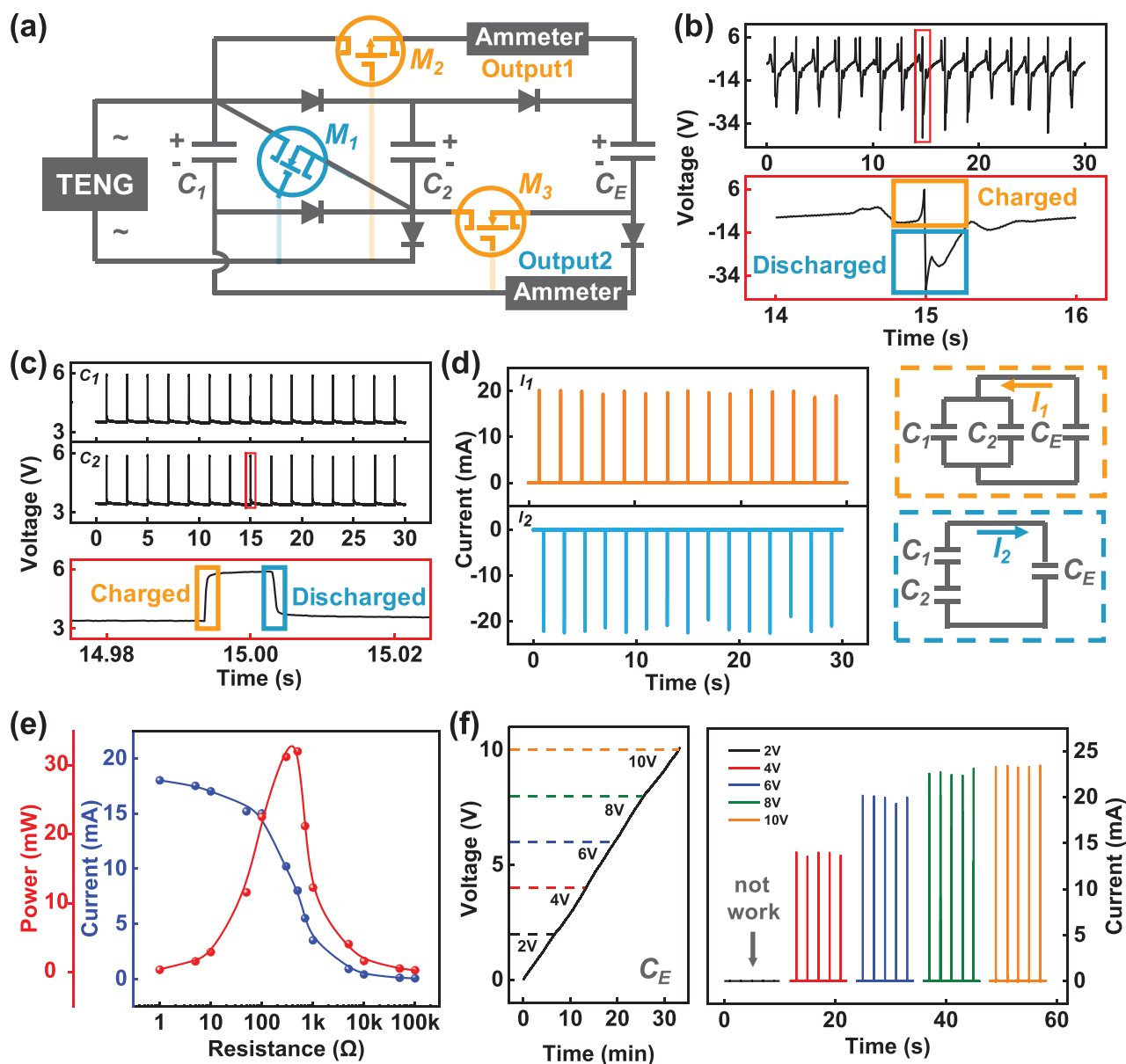


Figure 2. a) Detailed circuit diagram of the CEC integrated with the TENG. b) Voltage that the TENG inputs into the charge excitation system. c) Voltage change on the capacitors C_1 and C_2 in the circuit. d) Current profiles and directions of the Outputs 1 and 2 of the charge excitation system. e) Peak current and peak power with respect to the load resistance for the charge excitation TENG. The vibration frequency and the voltage value on the C_E were, respectively, fixed to be 0.6 Hz and 6 V. f) Voltage curve when the TENG first charges C_E and the relevant output current when C_E is charged to different voltage values.

Figure 3a. The influences of the water wave frequency and wave height on the TENG outputs were investigated, because they were found to be the two most crucial factors in our previous studies.^[36] The trend of the TENG output current at different water wave frequencies from 0.2 to 1.4 Hz is shown in Figure 3b, when fixing the wave height as 10 cm and the voltage value on C_E as 6 V. In this figure, only the current of Output 1 was measured, whereas the current of Output 2 under the optimal water wave condition is revealed in Figure S6, Supporting Information. As the water wave frequency increases, the output current first increases then decreases, reaching the maximum value of 25.1 mA at 0.6 Hz. Furthermore, the output power arrives at the

peak value of 25.8 mW with the matched resistance of 300 Ω at the frequency of 0.6 Hz, as shown in Figure 3c, and the corresponding power density is calculated to be 49.3 $W m^{-3}$. The initial increase of power is due to faster compression of the multilayered units inside the spherical TENG, which improves the voltage input into the CEC and decreases the resistance of MOSFETs when they are turned on. However, higher frequency will result in larger switching loss of the MOSFETs in the CEC, limiting this circuit to be only suitable for low frequency motions. In our previous work, the best water wave frequency was found to be 1.0 Hz,^[36] which is different from 0.6 Hz in this work. The drop is due to higher power consumption of the CEC

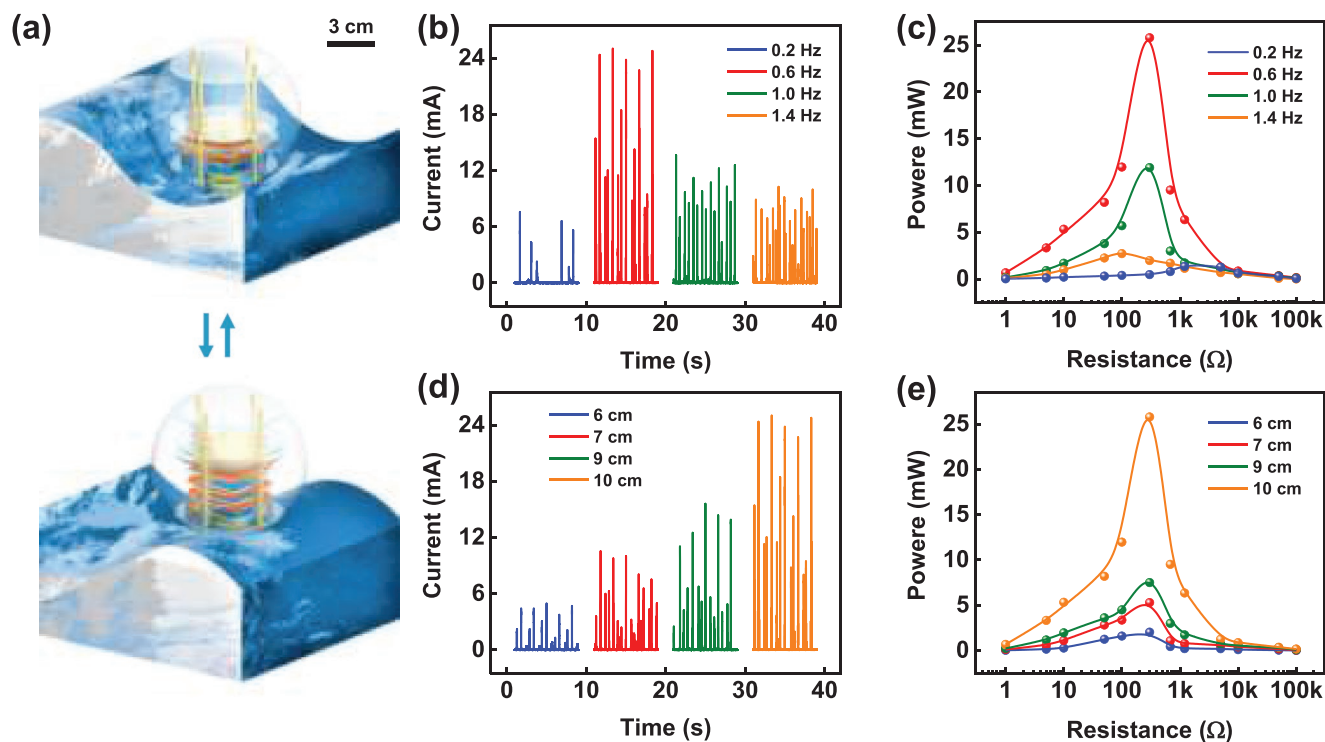


Figure 3. a) Schematic scene of a single TENG vibrating in water waves created by the standard wave tank equipment. b) Output current c) output power-resistance profiles of the TENG integrated with the CEC at various water wave frequencies. The wave height and the voltage on C_E are maintained as 10 cm and 6 V. d) Output current e) output power-resistance relationships at various wave heights. The wave frequency and the voltage on C_E were fixed as 0.6 Hz and 6 V.

at higher frequency. On the other hand, at the fixed wave frequency of 0.6 Hz, the output current and power of the TENG at various wave heights from 6 to 10 cm were measured as shown in Figure 3d,e. Obviously, the current and power of the TENG both increase with increasing the wave height, because of the increased voltage input into the CEC and decreased energy loss at a higher motion amplitude of water waves.

For adapting large-scale harvesting of water wave energy in future, the researches on TENG networks are essential. In this work, a hexagonal TENG network with seven spherical TENG units linked by rigid strings was fabricated, presented in Figure 4b. The schematic diagram of the connection manner between the CECs and the units in the TENG network is shown in Figure 4a. Each TENG unit is first connected to a CEC, respectively, to improve its output performance, and its AC output is converted to DC output at the same time. If TENG units in the network are first connected with each other through rectifier bridges, the DC output cannot make the CEC properly work and even damages the components in it. Then, these seven TENG units are directly connected in parallel through the Output 1 of the CECs without rectified bridges, while the Output 2 of each CEC must ensure short-circuit state. Otherwise, the Output 1 and Output 2 will affect each other, causing the CECs unable to work properly. The same function can also be realized by shorting Output 1 and connecting Output 2 in parallel, and the output performance of the TENG network in this case under the optimal water wave conditions is shown in Figure S7, Supporting Information.

The output performance of the TENG network with the CECs under different water wave frequencies (Figure 4c,d) and heights (Figure 4e,f) were systematically studied, and the output current values are summarized in the 3D graph for intuitiveness (Figure 4g). The trends of the output current and output power are identical with the former single TENG, and the maximum current of 24.5 mA and maximum power of 24.6 mW are also obtained at the wave frequency of 0.6 Hz and the wave height of 10 cm. However, the matched resistance under all water wave conditions decreases compared to the single TENG, resulting from the increase of capacitance. Although the maximum values of the outputs are not multiplied by the TENG network due to the asynchronous movement of each TENG unit, the density of output current peaks is significantly increased. The charging performance of the TENG network with the CECs to various load capacitors from 22 μF to 4.7 mF in 30 s was investigated, as presented in Figure 4h. The charging voltage for each capacitance first rises at a rapid speed, and then slowly saturates. For smaller capacitance, the charging speed is faster, and a larger voltage can be achieved. In order to reveal the effect of the CECs on the TENG network, the comparison graph of charging a 4.7 mF capacitor directly or integrated with the CECs is shown in Figure S8, Supporting Information, exhibiting 86 times improvement of charging speed by the CECs.

Integrated with the CECs, the high-output TENG network enriches the feasibility of practical harvesting of water wave energy. In the following experiments, two specific applications

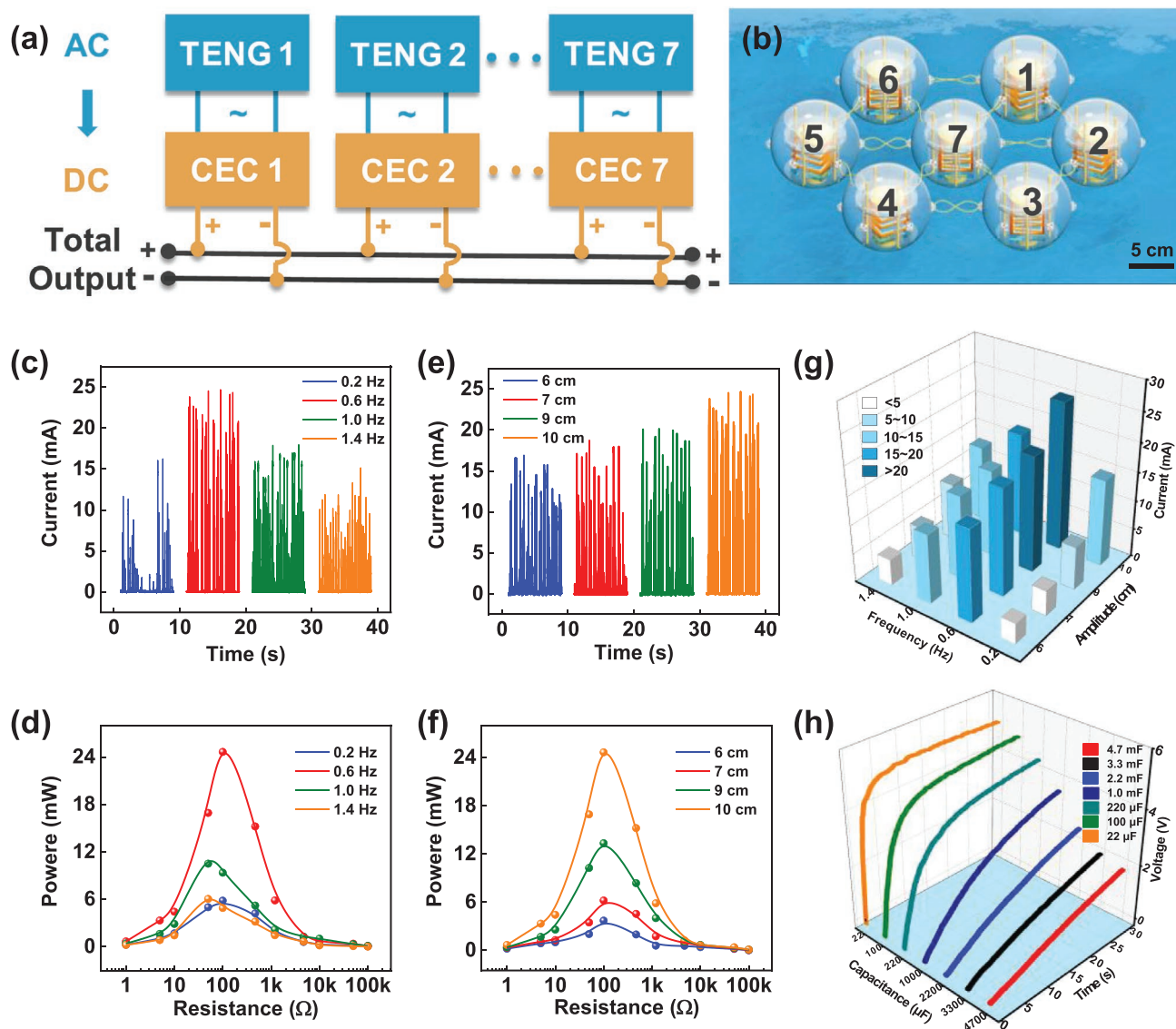


Figure 4. a) Sketch of the charge excitation TENG network in which each unit is, respectively, connected by one CEC followed by a parallel connection. b) Schematic representation of the hexagonal TENG network containing seven spherical TENGs linked by rigid strings floating on the ocean surface. c) Output current and d) output power-resistance profiles of the charge excitation TENG network for various wave frequencies at the wave height of 10 cm and voltage of 6 V on the C_E . e) Output current and f) power-resistance relationships of the charge excitation TENG network at various wave heights with the frequency of 0.6 Hz and voltage of 6 V on C_E . g) 3D graph summarizing the effects of wave frequency and height on the average output current peaks. h) Charging voltage curves to various capacitors for the TENG network with the CECs.

were demonstrated, the conception of which is depicted in **Figure 5a**. In order to meet the electricity demands of the subsequent applications, the system first charges a capacitor (100 μF) to convert the pulsed outputs into constant outputs. Utilizing this constant direct current, a thermometer can continuously measure the temperature of the environment autonomously, and the values can be displayed at a liquid crystal display (LCD) screen in real time. **Figure 5b** is the voltage curve on the thermometer driven by the charge excitation TENG network working under the optimal water wave conditions. The voltage first reaches the value of 2 V rapidly, at which the thermometer starts to work normally. Then the voltage is maintained between 1.8 and 2 V, so the thermometer is able to work

constantly until the TENG network stops working. The photograph of the lighted LCD screen of the thermometer is shown in the inset of **Figure 5b**, and the process of this application was recorded in Video S1, Supporting Information.

Besides the thermometer, a wireless communication system with a mobile phone was designed to demonstrate the useful applications of the charge excitation TENG network, whose detailed circuit diagram is depicted in **Figure S9**, Supporting Information. After the TENG network with CECs charges a capacitor (470 μF), a wireless transmitter is connected to the system. If this wireless transmitter sends an RF signal, the corresponding receiving terminal will work immediately and control the single chip microcomputer to transmit data to the

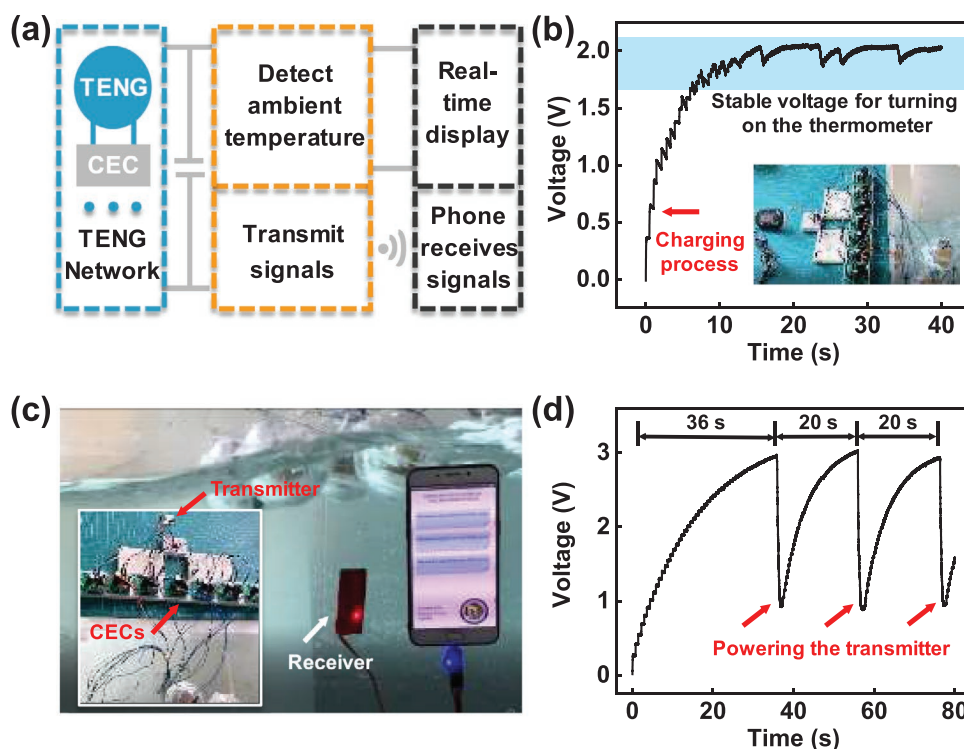


Figure 5. a) Framework for the self-powered marine information detection and wireless communication system driven by the charge excitation TENG network. b) Voltage profile on the thermometer and the photograph of the LCD screen. c) Photograph of the transmitted information displayed on the mobile phone screen. d) Voltage curve on the wireless transmitter for several consequent transmitting cycles.

mobile phone through the serial ports. A special compiled program for visually displaying information sent by the TENG network has been already installed into this mobile phone. Figure 5d shows the voltage profile on the wireless transmitter driven by the charge excitation TENG network for several consequent transmitting cycles. Once the voltage reaches 3 V, the transmitter consumes electrical power and emits signals. The high-output TENG network is able to quickly fill the voltage drop and power the transmitter to send wireless signals again. After the pre-starting stage, the TENG network transmits a signal to the mobile phone almost every 20 s. The mobile phone receives the data and processes them, and the photograph of the received information displayed on the mobile phone screen is exhibited in Figure 5c. Due to the space limitation, we only show the case for about 0.5 m away. Actually, the transmission distance of the wireless signals is more than 10 m. The detailed experiment process can be found in Video S2, Supporting Information.

3. Conclusion

In summary, we designed and fabricated a charge excitation circuit to achieve high-output TENGs for effectively harvesting water wave energy, which is completely different from previous voltage double circuits. The addition of MOSFETs and C_E absolutely change the way of ordinary voltage double circuits to multiply the voltage. The working mechanism of the CEC was elaborated by measuring voltage values on various parts of

the system. The output performance of the charge excitation TENG was also studied. When triggered by real water waves, the outputs of the charge excitation TENG were found to be controlled by the water wave frequency and amplitude. Under the optimal water wave condition with the frequency of 0.6 Hz and amplitude of 10 cm, the maximum output current and power can reach 25.1 mA and 25.8 mW, respectively. Furthermore, a TENG network integrated with the CECs was proposed and fabricated to harvest the water wave energy, presenting a maximum output current of 24.5 mA and power of 24.6 mW. The CEC improves both the output current and power of TENG, which is the most important difference from ordinary voltage double circuit that can only increase the output voltage. Finally, the high-output TENG network was utilized to drive a thermometer to work continuously and realize the wireless communication with a mobile phone for remote environmental monitoring.

4. Experimental Section

Fabrication of the Hexagonal TENG Network: First, the spherical TENG unit devices in the TENG network were fabricated. As the main part of the spherical TENG, the multilayered structure contains seven basic contact-separation mode TENG units, which are held by a 50 μm -thick Kapton strip (32 cm \times 4 cm). One contact-separation TENG unit consists of an Al foil (3 cm \times 3 cm) as an electrode and another same Al foil bonded with a 12.5 μm -thick FEP film (3 cm \times 3 cm). Electrons were injected onto the surfaces of FEP films at a polarization voltage of 5 kV. The multilayered structure was supported by four springs and pressed by a copper block. The design of the spring-assisted structure and other

fabrication details can be found in the previous work.^[36] Second, the spherical TENGs were sealed and waterproofed by using the tile cement for working in water environment. Finally, seven spherical TENGs were arranged in a hexagonal structure with a diameter of 40 cm and linked by rigid strings. Each spherical TENG was first integrated with a CEC separately to achieve high outputs, and then electrically connected in parallel to each other.

Electric Measurements of the TENG Device: The electric outputs of the TENG device were measured under regular water waves generated by a standard wave tank equipment reported previously,^[18] which contained a wave generating mechanism and a rebound wave absorber. The output current, transferred charge, charging voltage of the TENGs integrated with the CEC, and the voltage change on capacitors inside the CEC were obtained by a current preamplifier (Keithley 6514 System Electrometer).

Supporting Information

Supporting Information is available from the Wiley Online Library or from the author.

Acknowledgements

X.L. and T.J. contributed equally to this work. Supports from the National Key R & D Project from Minister of Science and Technology (2016YFA0202704), National Natural Science Foundation of China (Grant Nos. 51432005, 51702018, and 51561145021), and Youth Innovation Promotion Association, CAS, are appreciated. The authors also thank Kai Han and Pengfei Chen for device fabrications and measurements.

Conflict of Interest

The authors declare no conflict of interest.

Keywords

blue energy, charge excitation circuits, triboelectric nanogenerators, triboelectric nanogenerator networks, wave energy harvesting

Received: June 29, 2020

Revised: July 30, 2020

Published online:

- [1] J. P. Painuly, *Renew. Energy* **2001**, *24*, 73.
- [2] S. P. Beeby, R. N. Torah, M. J. Tudor, P. Glynne-Jones, T. O'Donnell, C. R. Saha, S. Roy, *J. Micromech. Microeng.* **2007**, *17*, 1257.
- [3] Z. L. Wang, J. Chen, L. Lin, *Energy Environ. Sci.* **2015**, *8*, 2250.
- [4] X. Wang, Y. Yang, *Nano Energy* **2017**, *32*, 36.
- [5] Z. Wu, H. Guo, W. Ding, Y. C. Wang, L. Zhang, Z. L. Wang, *ACS Nano* **2019**, *13*, 2349.
- [6] F. R. Fan, Z. Q. Tian, Z. L. Wang, *Nano Energy* **2012**, *1*, 328.
- [7] Y. Yao, T. Jiang, L. Zhang, X. Chen, Z. Gao, Z. L. Wang, *ACS Appl. Mater. Interfaces* **2016**, *8*, 21398.
- [8] L. Xu, T. Jiang, P. Lin, J. J. Shao, C. He, W. Zhong, X. Y. Chen, Z. L. Wang, *ACS Nano* **2018**, *12*, 1849.
- [9] J. Wang, Z. Wu, L. Pan, R. Gao, B. Zhang, L. Yang, H. Guo, R. Liao, Z. L. Wang, *ACS Nano* **2019**, *13*, 2587.
- [10] Z. L. Wang, *Faraday Discuss.* **2014**, *176*, 447.
- [11] Z. L. Wang, *Mater. Today* **2017**, *20*, 74.
- [12] G. Zhu, Y. S. Zhou, P. Bai, X. S. Meng, Q. S. Jing, J. Chen, Z. L. Wang, *Adv. Mater.* **2014**, *26*, 3788.
- [13] M. Xu, T. Zhao, C. Wang, S. L. Zhang, Z. Li, X. Pan, Z. L. Wang, *ACS Nano* **2019**, *13*, 1932.
- [14] G. Cheng, H. W. Zheng, F. Yang, L. Zhao, M. L. Zheng, J. J. Yang, H. F. Qin, Z. L. Du, Z. L. Wang, *Nano Energy* **2018**, *44*, 208.
- [15] D. Liu, B. D. Chen, J. An, C. Y. Li, G. X. Liu, J. J. Shao, W. Tang, C. Zhang, Z. L. Wang, *Nano Energy* **2020**, *73*, 104819.
- [16] Y. X. Bian, T. Jiang, T. X. Xiao, W. P. Gong, X. Cao, Z. N. Wang, Z. L. Wang, *Adv. Mater. Technol.* **2018**, *3*, 1700317.
- [17] Z. R. Liu, J. H. Nie, B. Miao, J. D. Li, Y. B. Cui, S. Wang, X. D. Zhang, G. R. Zhao, Y. B. Deng, Y. H. Wu, Z. Li, L. L. Li, Z. L. Wang, *Adv. Mater.* **2019**, *31*, 1807795.
- [18] J. An, Z. M. Wang, T. Jiang, X. Liang, Z. L. Wang, *Adv. Funct. Mater.* **2019**, *29*, 1904867.
- [19] Y. W. Feng, T. Jiang, X. Liang, J. An, Z. L. Wang, *Appl. Phys. Rev.* **2020**, *7*, 021401.
- [20] X. Liang, T. Jiang, G. X. Liu, Y. W. Feng, C. Zhang, Z. L. Wang, *Energy Environ. Sci.* **2020**, *13*, 277.
- [21] X. Liang, T. Jiang, G. Liu, T. Xiao, L. Xu, W. Li, F. Xi, C. Zhang, Z. L. Wang, *Adv. Funct. Mater.* **2019**, *29*, 1807241.
- [22] K. I. Park, C. K. Jeong, N. K. Kim, K. J. Lee, *Nano Converg.* **2016**, *3*, 12.
- [23] J. H. Nie, Z. W. Ren, L. Xu, S. Q. Lin, F. Zhan, X. Y. Chen, Z. L. Wang, *Adv. Mater.* **2020**, *32*, 1905696.
- [24] J. H. Nie, Z. M. Wang, Z. W. Ren, S. Y. Li, X. Y. Chen, Z. L. Wang, *Nat. Commun.* **2019**, *10*, 2264.
- [25] X. Chen, L. X. Gao, J. F. Cheng, S. Lu, H. Zhou, T. T. Wang, A. B. Wang, Z. F. Zhang, S. F. Guo, X. J. Mu, Z. L. Wang, Y. Yang, *Nano Energy* **2020**, *69*, 104440.
- [26] X. D. Yang, L. Xu, P. Lin, W. Zhong, Y. Bai, J. Luo, J. Chen, Z. L. Wang, *Nano Energy* **2019**, *60*, 404.
- [27] J. Y. Wang, P. Lu, H. Y. Guo, B. B. Zhang, R. R. Zhang, Z. Y. Wu, C. S. Wu, L. J. Yang, R. J. Liao, Z. L. Wang, *Adv. Energy Mater.* **2019**, *9*, 1802892.
- [28] T. X. Xiao, T. Jiang, J. X. Zhu, X. Liang, L. Xu, J. J. Shao, C. L. Zhang, J. Wang, Z. L. Wang, *ACS Appl. Mater. Interfaces* **2018**, *10*, 3616.
- [29] S. Y. Li, J. H. Nie, Y. X. Shi, X. L. Tao, F. Wang, J. W. Tian, S. Q. Lin, X. Y. Chen, Z. L. Wang, *Adv. Mater.* **2020**, *32*, 2001307.
- [30] S. Y. Li, Y. Fan, H. Q. Chen, J. H. Nie, Y. X. Liang, X. L. Tao, J. Zhang, X. Y. Chen, E. G. Fu, Z. L. Wang, *Energy Environ. Sci.* **2020**, *13*, 896.
- [31] B. Y. Lee, D. H. Kim, J. Park, K. I. Park, K. J. Lee, C. K. Jeong, *Sci. Tech. Adv. Mater.* **2019**, *20*, 758.
- [32] R. D. I. G. Dharmasena, K. D. G. I. Jayawardena, C. A. Mills, J. H. B. Deane, J. V. Anguita, R. A. Dorey, S. R. P. Silva, *Energy Environ. Sci.* **2017**, *10*, 1801.
- [33] W. Liu, Z. Wang, G. Wang, G. Liu, J. Chen, X. Pu, Y. Xi, X. Wang, H. Guo, C. Hu, Z. L. Wang, *Nat. Commun.* **2019**, *10*, 1426.
- [34] L. Xu, T. Z. Bu, X. D. Yang, C. Zhang, Z. L. Wang, *Nano Energy* **2018**, *49*, 625.
- [35] W. Liu, Z. Wang, G. Wang, Q. Zhen, W. He, L. Liu, X. Wang, Y. Xi, H. Guo, C. Hu, Z. L. Wang, *Nat. Commun.* **2020**, *11*, 1883.
- [36] T. X. Xiao, X. Liang, T. Jiang, L. Xu, J. J. Shao, J. H. Nie, Y. Bai, W. Zhong, Z. L. Wang, *Adv. Funct. Mater.* **2018**, *28*, 1802634.
- [37] Z. L. Wang, T. Jiang, L. Xu, *Nano Energy* **2017**, *39*, 9.